A&A 619, A146 (2018)
https://doi.org/10.1051/0004-6361/201833936

Astronomy & Astrophysics

From solar to stellar brightness variations

The effect of metallicity

V. Witzke[1], A. I. Shapiro[1], S. K. Solanki[1,2], N. A. Krivova[1], and W. Schmutz[3]

[1] Max Planck Institute for Solar System Research, Justus-von-Liebig-Weg 3, 37077 Göttingen, Germany
e-mail: witzke@mps.mpg.de
[2] School of Space Research, Kyung Hee University, Yongin, Gyeonggi 446-701, Republic of Korea
[3] Physikalisch-Meteorologishes Observatorium Davos, World Radiation Center, 7260 Davos Dorf, Switzerland

Received 24 July 2018 / Accepted 30 August 2018

ABSTRACT

Context. Comparison studies of Sun-like stars with the Sun suggest an anomalously low photometric variability of the Sun compared to Sun-like stars with similar magnetic activity. Comprehensive understanding of stellar variability is needed to find a physical reason for this observation.
Aims. We investigate the effect of metallicity and effective temperature on the photometric brightness change of Sun-like stars seen at different inclinations. The considered range of fundamental stellar parameters is sufficiently small so the stars investigated here still count as Sun-like or even as solar twins.
Methods. To model the brightness change of stars with solar magnetic activity, we extended a well-established model of solar brightness variations based on solar spectra, Spectral And Total Irradiance REconstruction (SATIRE), to stars with different fundamental parameters. For this we calculated stellar spectra for different metallicities and effective temperature using the radiative transfer code ATLAS9.
Results. We show that even a small change (e.g. within the observational error range) of metallicity or effective temperature significantly affects the photometric brightness change compared to the Sun. We find that for Sun-like stars, the amplitude of the brightness variations obtained for Strömgren $(b + y)/2$ reaches a local minimum for fundamental stellar parameters close to the solar metallicity and effective temperature. Moreover, our results show that the effect of inclination decreases for metallicity values greater than the solar metallicity. Overall, we find that an exact determination of fundamental stellar parameters is crucially important for understanding stellar brightness changes.

Key words. stars: variables: general – stars: activity – stars: atmospheres – stars: fundamental parameters – radiative transfer

1. Introduction

Stellar activity is caused by magnetic fields emerging from below the stellar surface and evolving due to the complex interaction of gas dynamics and magnetic flux. The resulting concentrations of magnetic fields produce a variety of phenomena, including spots and faculae that lead to darkening and brightening on the stellar surface. Such emerging magnetic features can be directly observed on the Sun, due to its exclusive location, and thus have been studied in great detail (see e.g. Solanki et al. 2006). In contrast, stellar activity can be accessed only by indirect manifestations of the surface structures, i.e. spectroscopic and brightness variations, as well as proxies of magnetic heating of the stellar atmosphere, and chromospheric Ca II and coronal X-ray emission.

Stellar long-term variability investigations were launched in the 1950s by several observatories, such as the Lowell Observatory, to monitor variations in photometric brightness and chromospheric activity (see Wilson 1978; Baliunas et al. 1995; Lockwood et al. 2013, and references therein). These studies provide an observational survey of the relation between photometric variations and chromospheric activity among lower main-sequence stars (Radick et al. 1998, 2018; Lockwood et al. 2007; Hall et al. 2009), and led to several important findings. First, the photometric variability is stronger for stars with higher magnetic activity. Second, it was found that among stars with a certain chromospheric activity level a transition from faculae-dominated to spot-dominated stellar photometric variations occurs (Lockwood et al. 2007; Hall et al. 2009) such that the correlation between Ca II and the photometry displayed by the Sun becomes an anticorrelation for more active stars. Third, investigations comparing the Sun with other main-sequence stars (Lockwood et al. 2007, 2013) showed that solar brightness variability over the 11-year activity cycle appears to be anomalously low compared with stars of near-solar magnetic activity.

This last observation was used to suggest that historical solar variability and consequently the solar role in pre-industrial climate change might have been significantly greater than thought before (see e.g. Lean et al. 1992; Shapiro et al. 2011; Judge et al. 2012; Solanki et al. 2013). Another recently proposed explanation (Shapiro et al. 2016) is based on the fact that solar brightness variability is caused by a delicate balance between dark and bright magnetic features. This balance is sensitive to the combination of stellar fundamental parameters that define properties of magnetic features, i.e. effective temperature, metallicity, and surface gravity. Consequently, stars with slightly different fundamental parameters can show significantly altered parameters, e.g. higher brightness variations. So far this hypothesis could not be tested due to the absence of reliable stellar atmospheric models for magnetic features that has hindered the

development of quantitative models of stellar brightness variability for a long time.

In contrast to other stars, accurate model atmospheres of quiet regions and magnetic features exist for the Sun. The variability of Sun-like stars can reasonably be assumed to be based on the same mechanisms as on the Sun, where the processes that are responsible can be observed in detail. Therefore, it is possible to extend solar irradiance models (see Ermolli et al. 2013; Solanki et al. 2013, and references therein) to investigate Sun-like stars. Previous studies suggested several approaches depending on the issue of interest. For example, the effect of inclination for stars observed out of their equatorial plane on the photometric variability (Schatten 1993; Knaack et al. 2001; Vieira et al. 2012; Shapiro et al. 2014) was studied and a potential increase in variability was found for large inclinations. Lanza et al. (2009) developed different brightness variability models that account for active regions, but which have at least eleven free parameters, to analyse and fit observed light curves. Moreover, the correlation between the faculae and spot-dominated stellar variability and magnetic activity was investigated by modelling a hypothetical Sun at different activity levels and extrapolating the surface coverage by solar magnetic features to another mean chromospheric activity level (Shapiro et al. 2014). These investigations can explain the activity dependence of variability as well as the transition from faculae- to spot-dominated stars; however, they do not address the anomalously low brightness variability of the Sun, which remains a long-standing puzzle.

Generally, stars are characterised as Sun-like or even solar twins if their fundamental stellar parameters are close to the solar parameters. While such stars are close to the solar case, no star has the identical set of fundamental stellar parameters. Here the goal is to shed light on the role of several stellar fundamental parameters for stellar brightness change, in particular different metallicities and effective temperatures. For this, we extended the successful brightness variations model Spectral And Total Irradiance REconstruction (SATIRE; Fligge et al. 2000; Krivova et al. 2003) to Sun-like stars with different fundamental stellar parameters. Thus, we take advantage of building on the successful existing solar models that have been developed for decades and agree accurately with the solar observations. Whereas most stellar brightness variation studies assumed solar contrast of magnetic features, we took a different path. Our novel approach is based on calculating the spectral contrasts of spot umbrae, spot penumbrae, and faculae to the quiet stellar region depending on stellar fundamental parameters. This allows us to investigate the influence of stellar fundamental parameters, for example metallicity and effective temperature, on stellar brightness variations. Here, we limited our study to stars with the same surface distribution of magnetic features as the solar case. The main goal is to investigate stellar brightness change, in particular in the Strömgren b and y filters and the *Kepler* pass-band, on the timescale of magnetic activity cycles.

This paper is structured as follows. In Sect. 2 our theoretical approach is described. In Sect. 3 we present our results of the effect of the metallicity, inclination, and effective temperature on stellar brightness change. Finally, we provide a summary and draw conclusions in Sect. 4.

2. Model: From the Sun to stars

In this study we focus on stellar photometric brightness change on the magnetic activity cycle timescale, which for the Sun is approximately 11 years. Another important timescale is the rotational timescale, which will be investigated separately in a follow-up paper. To obtain a time dependent spectrum the observed magnetic feature distributions of solar cycle 23 are used, which was a cycle of intermediate strength. The effect of the cycle strength on the brightness variations was investigated in Shapiro et al. (2014), and here we used a representative cycle for which we have good measurements of solar surface magnetic field. The typical distributions of faculae and spots on the solar surface during the maxima and minima of the solar cycle are shown in Fig. 1, together with the time-evolution of the solar irradiance in Strömgren filter b. The difference between the years 2000 and 2008, indicated by red horizontal lines in the bottom panel of Fig. 1, is taken here to represent the brightness change on the activity cycle timescale.

2.1. Photometric brightness change

The SATIRE model that we describe here was used to compute the photometric brightness change. The SATIRE model separately accounts for the quiet stellar regions, star spot umbral, star spot penumbral, and facular components (Krivova et al. 2003). Following the detailed description in Shapiro et al. (2014) the spectral flux can be decomposed into two main contributions:

$$F(\lambda) = F_{\rm Q}(\lambda) + F_{\rm m}(\lambda), \tag{1}$$

where Q denotes the quiet part of the stellar surface, m is associated with different magnetic features, and λ is the wavelength. Then, the disc integrated flux $F_{\rm Q}(\lambda)$ is obtained by integrating

$$F_{\rm Q}(\lambda) = \int_0^1 I_{\rm Q}(\lambda,\mu)\omega(\mu){\rm d}\mu, \tag{2}$$

where $\omega(\mu) = 2\pi\mu(r_{\rm star}/d_{\rm star})^2$ is a weighting function with the stellar radius, $r_{\rm star}$, and the distance between the star and observer, $d_{\rm star}$. The considered emergent intensity, $I_{\rm Q}(\lambda,\mu)$, also depends on μ, which is the cosine of the angle between the observer's direction and the local stellar radius. The magnetic features contribute through their contrast $I_{\rm m}(\lambda,\mu) - I_{\rm Q}(\lambda,\mu)$ to the stellar brightness

$$F_{\rm m}(\lambda) = \int_0^1 \sum_{\rm m} \alpha_{\rm m}(\mu)\left(I_{\rm m}(\lambda,\mu) - I_{\rm Q}(\lambda,\mu)\right)\omega(\mu){\rm d}\mu, \tag{3}$$

where the fractional coverage of the ring at the corresponding μ on the stellar disc is given by the functions $\alpha_{\rm m}(\mu)$. In this formulation the coverage at the stellar disc centre is associated with $\alpha_{\rm m}(\mu = 1)$ and at the limb with $\alpha_{\rm m}(\mu = 0)$. In order to gain a more detailed understanding of separate contributions from faculae and spots, $F_{\rm m}$ can be further decomposed. The facular spectral flux is defined as

$$F_{\rm Fac}(\lambda) = \int_0^1 \alpha_{\rm Fac}(\mu)\left(I_{\rm Fac}(\lambda,\mu) - I_{\rm Q}(\lambda,\mu)\right)\omega(\mu){\rm d}\mu, \tag{4}$$

whereas the spectral flux from spots consists of both the spot umbra and spot penumbra components:

$$\begin{aligned} F_{\rm spot}(\lambda) \;=\; & \int_0^1 \alpha_{\rm Pen}(\mu)\left(I_{\rm Pen}(\lambda,\mu) - I_{\rm Q}(\lambda,\mu)\right)\omega(\mu){\rm d}\mu \\ & + \int_0^1 \alpha_{\rm Umb}(\mu)\left(I_{\rm Umb}(\lambda,\mu) - I_{\rm Q}(\lambda,\mu)\right)\omega(\mu){\rm d}\mu. \end{aligned} \tag{5}$$

The solar intensities, $I(\lambda,\mu)$, and solar surface coverages, $\alpha_{\rm m}(\mu)$, fully determine the solar Sun. In previous investigations the

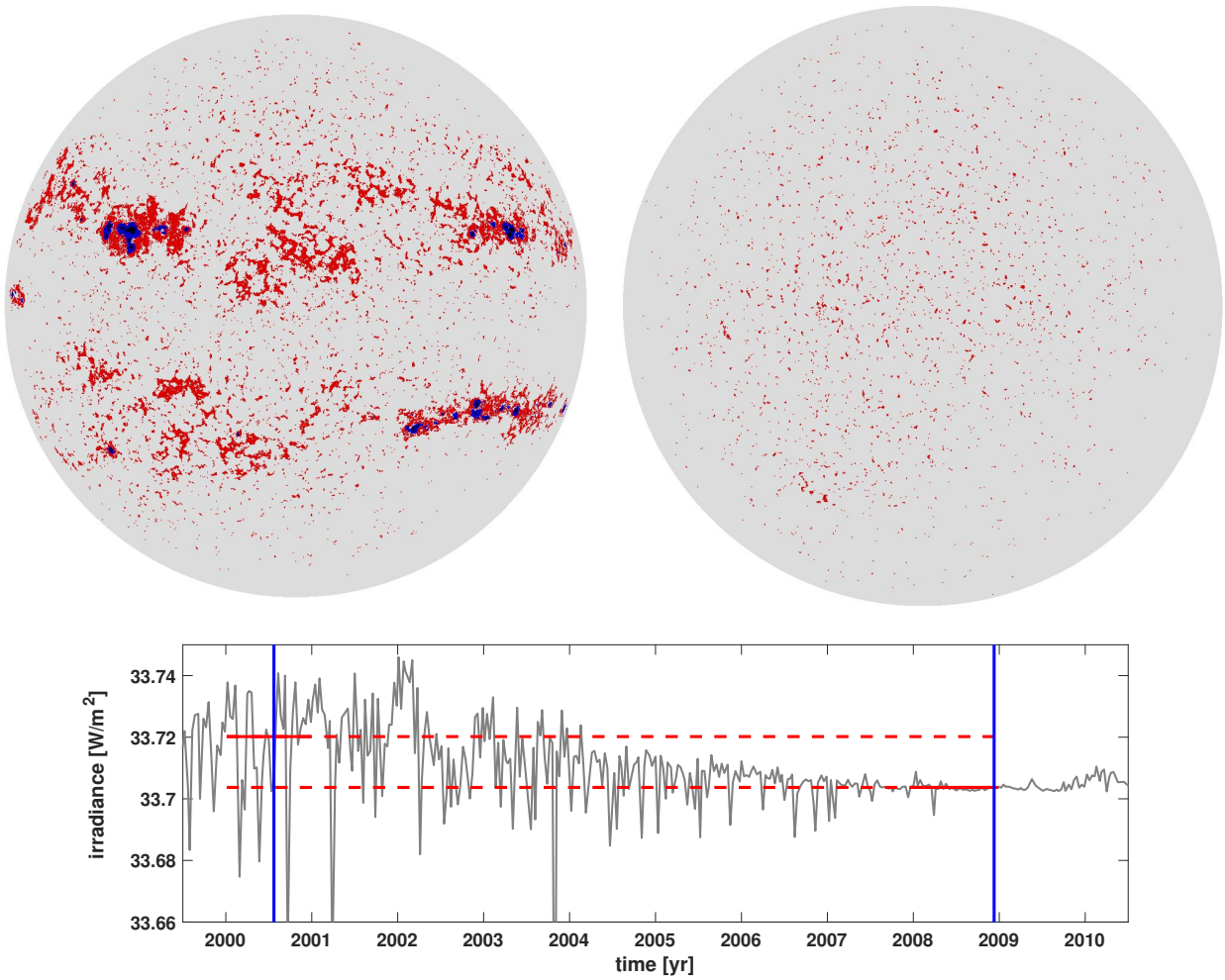

Fig. 1. Distribution of magnetic features on the solar surface (*upper row*) and computed irradiance variations (*lower panel*). *Upper plots*: black areas represent umbra, blue regions denote penumbra, and red areas are faculae. *Top left*: 11 July 2000. *Top right*: 1 Dec. 2008. *Lower plot*: solar irradiance in Strömgren *b* filter. Here we normalise the total amount of spectral energy to one AU. The vertical blue lines represent the times of the two upper plots. The two horizontal lines represent the average irradiance levels in the years 2000 and 2008.

magnetic feature coverage, $\alpha_{\rm m}(\mu)$, was varied to model different stars (Knaack et al. 2001; Lanza et al. 2009; Shapiro et al. 2014), whereas the emergent intensities, $I_{\rm m}(\lambda,\mu)$ and $I_{\rm Q}(\lambda,\mu)$, and thus the contrasts of the magnetic features were fixed to be as on the Sun. Since the aim of this investigation is to understand potential differences between brightness changes on a hypothetical Sun with slightly different fundamental parameters, we utilise a complementary approach and use the same coverage of stellar features as for the solar case, but contrasts of the magnetic features and their centre-to-limb variations (CLVs) will be adopted by recalculating the emergent intensities from the quiet and magnetic stellar regions.

2.2. Radiative transfer model

In this study we are interested in the amplitude of solar cycle brightness change, defined here as the difference between annually averaged solar brightness in 2000 (cycle maximum) and 2008 (cycle minimum). To obtain the brightness change using Eqs. (1)–(3), the emergent spectra for the different stellar components are needed. They can be calculated by solving the radiative transport equation for the corresponding atmospheric models. For the photospheric layers of the quiet Sun, spot umbra, and spot penumbra such atmospheric models are often computed assuming radiative equilibrium, while convection is included through mixing length theory (Böhm-Vitense 1958). The faculae models are semi-empirical (Vernazza et al. 1981; Lemaire et al. 1981; Fontenla et al. 1993, 2006), i.e. they are constructed to match their output to solar observations recorded at intermediate spatial resolution (Vernazza et al. 1981). Thus, faculae models are not in radiative equilibrium. Even though these models do not account for the geometric properties of magnetic features such as hot walls in magnetic flux tubes (Solanki 1993; Steiner 2005), ensembles of which form network and faculae, they have been successfully used for many applications, in particular for modelling solar brightness variations (Solanki et al. 2013).

In order to obtain the emergent intensities across a wide range of wavelengths from the atmospheric models, we used the LTE spectral synthesis code ATLAS9 (Kurucz 1992; Castelli & Kurucz 1994). For the calculation of the stellar continuum opacities, the following contributors were taken into account: Free-free (ff) and bound-free (bf) transitions in H^-, H I, H_2^+, He I, He II, and He^-. In addition, ff and bf transitions for low to high temperature absorbers such as C, N, O, Ne, Mg, Al, and Si. Moreover, electron scattering and Rayleigh scattering on H I, He I, and H_2 were considered. ATLAS9 further

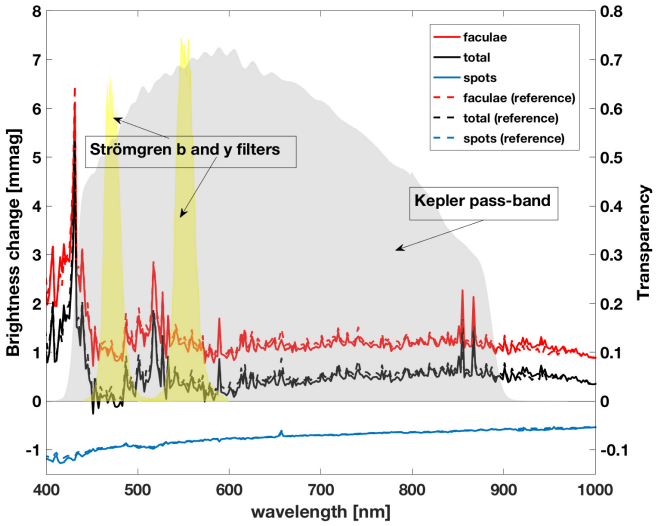

Fig. 2. Amplitude of solar cycle brightness change, here the difference between annually averaged solar brightness in 2000 (cycle max) and 2008 (cycle min) calculated with the SATIRE model (black). In addition, we plot the facular and spot components of the brightness change (red and blue). The grey shaded area indicates the spectral response function of the *Kepler* telescope measurements and the yellow shaded areas the Strömgren filters b and y (centred at 467 nm and 547 nm, respectively). Solid lines: Solar cycle brightness change calculated with the newest ATLAS9 code and ODFs. Dotted lines: Same, but using emergent spectra calculated by Unruh et al. (1999).

exploits opacity distribution functions (ODFs) to account for the opacity of millions of atomic and molecular spectral lines. The ODFs were generated by the code DFSYNTHE (Castelli 2005) for two microturbulence velocities of 1.5 km s^{-1} for the quiet stellar component and facular component, and of 2.0 km s^{-1} for the spot components, where a higher velocity was chosen to partly account for the large Zeeman splitting in the spots (Fontenla et al. 2006; Anderson et al. 2010). To account for the CLV, the emergent intensities, $I(\lambda, \mu)$, were calculated for 11 different μ values.

So far the SATIRE model has mainly made use of pre-calculated emergent spectra by Unruh et al. (1999) to successfully reconstruct the solar irradiance variations. For our purpose it is necessary to calculate these emergent spectra for different fundamental stellar parameters. The ATLAS9 code has evolved since Unruh et al. (1999) used it to compute the emergent spectra generally needed for the SATIRE model. Therefore, we recomputed the change in the solar spectrum between 2000 and 2008, as well as the facular and spot contributions to this change (shown in Fig. 2) by exploiting the newest ATLAS9 version together with recalculated ODFs for solar elemental composition taken from (Anders & Grevesse 1989). As our references we use the same atmospheric structures as Unruh et al. (1999) for the quiet sun, sun spots, and faculae. The thus obtained brightness changes agree very well with previous calculations by the SATIRE model based on the Unruh et al. (1999) spectra (see dotted lines in Fig. 2). The small deviations are due to updates incorporated over the last decades in the ATLAS9 and DFSYNTHE codes.

Now that we have validated the approach for the solar case, let us consider different metallicity values. These affect the spectrum in two ways. First, they change the strengths of atomic and molecular lines. Second, for a cool star, changed metallicity values influence the continuum opacity, due to the change in the concentration of electron donors. We consider these effects separately to judge the importance of each. In a first step, only the direct effect of the metallicity on the atomic and molecular lines was considered on its own. For this, we used the corresponding recalculated ODFs for the new metallicity, while keeping the atmosphere models used by Unruh et al. (1999) for the quiet Sun and magnetic features, thus neglecting the effect of a different metallicity on the atmosphere's structure and the electron concentration. The results of this approach are presented in Sect. 3.1. In the next step, the effect of lines and the change in the electron concentration along with the back-reaction of the changed radiation field on the atmospheric structure were considered. For this the ATLAS9 code provides a tool that self-consistently calculates 1D radiative equilibrium atmosphere models for different fundamental stellar parameters, i.e. effective temperature and metallicity. However, since the facular model was obtained semi-empirically, and no three-dimensional magnetohydrodynamic calculations (3D MHD) of magnetic features for different metallicities are currently available, the only option is to modify the reference facular model. The empirical modification of the atmospheric model for the faculae and the results of this approach are discussed in Sect. 3.2.

3. Results

To understand how fundamental stellar parameters affect the brightness change of a hypothetical Sun, we varied the metallicity, the inclination, and the effective temperature separately. We began our study by investigating the effect of metallicity on stellar brightness change. For that we first considered only the effect of Fraunhofer lines on the opacity (Sect. 3.1), where at this first stage we neglected the feedback on the atmospheric structure. We then analysed the combined effect due to Fraunhofer lines, changed electron number density, and changed stellar atmospheric structure (Sect. 3.2). The effect of inclination and effective temperature is considered in Sects. 3.3 and 3.4, respectively.

3.1. Direct effect of metallicity on Fraunhofer lines

On timescales greater than a day, brightness variations are determined by changes in the surface-area coverage by magnetic features (e.g. Solanki et al. 2013; Yeo et al. 2017). Therefore, the sum of the facular and star spot contributions is decisive for the amplitude of the photometric brightness change. Furthermore, Shapiro et al. (2015) showed that for the Sun, which is faculae-dominated, the main contribution to the brightness change on solar cycle timescales in the UV and visible spectral domains comes from the molecular and atomic lines that are present in the emergent spectra of faculae (see also Mitchell & Livingston 1991; Unruh et al. 2000). This has to do with the particular temperature structure of faculae. While their temperature is that of the quiet Sun near the Rosseland mean optical depth, $\tau_{\rm Ross}$, equal to unity, they are considerably hotter in the higher layers. Hence, at the disc centre their continuum contrast is relatively low, while in the cores of most spectral lines of neutral elements they are bright (Yeo et al. 2013). This is partly because the spectral lines of neutral atoms and molecules are weakened in faculae due to enhanced ionisation and dissociation, respectively.

The strengths of the lines (and especially of the weak unsaturated lines) depend on the metallicity, so that any change in the metallicity should affect the amplitude of the stellar brightness change. To quantify this effect we first computed emergent spectra by using ODFs for the relevant metallicities.

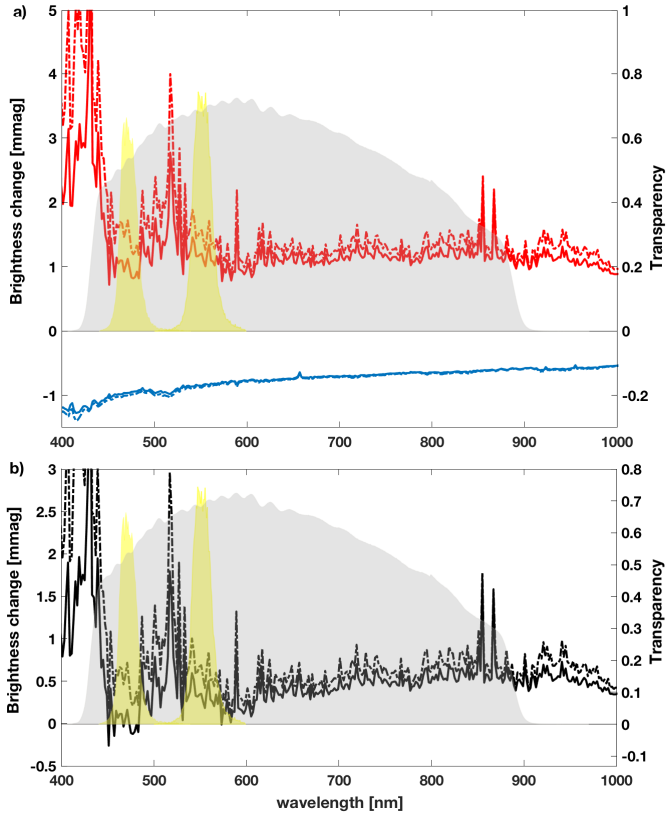

Fig. 3. *Panel a*: radiative flux difference between 2000 and 2008 for different atmospheric components and two metallicity values M/H. Facular (red) and spot (blue) contributions for M/H values of 0.0 (solid lines) and 0.2 (dashed lines). *Panel b*: same as in *panel a*, but now for the facular and spot contributions combined. The yellow and grey shaded areas are the same as in Fig. 2.

We calculated a set of ODFs with different metallicities, which are defined as

$$M/H = \log\left(\frac{(N_{\rm metals}/N_{\rm H})_{\rm star}}{(N_{\rm metals}/N_{\rm H})_{\rm Sun}}\right), \quad (6)$$

where $N_{\rm metalls}$ is the number density of all metals and $N_{\rm H}$ the number density of hydrogen. We started with the solar metallicity, $M/H = 0.0$, and the element composition by Anders & Grevesse (1989). To obtain metallicities in the range $-0.4 \leq M/H \leq 0.4$ in steps of 0.1, we scaled the ratio of all metals to hydrogen accordingly. The ODFs were then used together with the reference atmospheric models to calculate the emergent intensities for Eqs. (1)–(5) (SATIRE model). However, at this step the approach is not yet self-consistent. While the ratio of all metals to hydrogen is changed and thus the formation height of different lines is shifted, the H^- opacity, which is the main contributor to the continuum in the visible, remains unchanged because neither the electron density nor the temperature structure is recalculated. We note that in this approach, when only the metallicity for the line opacities is changed the effective temperature, $T_{\rm eff}$, is still somewhat affected; for example, for higher metallicities $T_{\rm eff}$ becomes lower due to stronger lines.

The brightness change computed in this way is shown in Fig. 3. Figure 3a shows the effect of an increased metallicity $M/H = 0.2$ for the facular and spot contributions separately, while Fig. 3b shows the effect on the overall brightness change. The solar case from Fig. 2 is also plotted for comparison. As

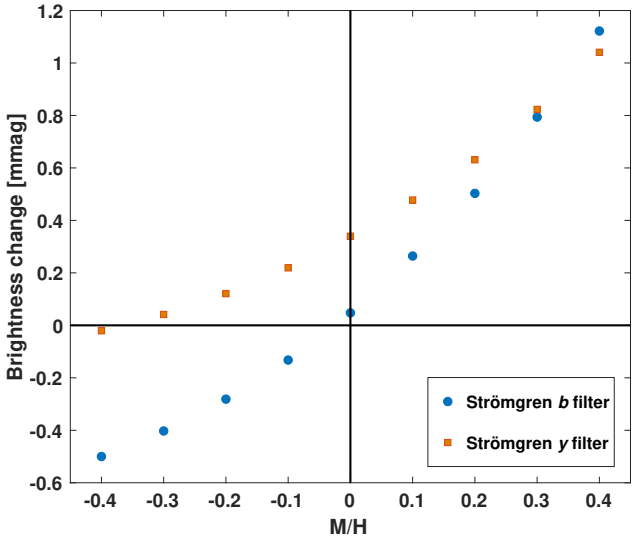

Fig. 4. Brightness change integrated over Strömgren b and y filters as a function of metallicity.

explained earlier in this section, the main reason why the Sun is brighter during activity cycle maximum are the weaker spectral lines in the faculae (Shapiro et al. 2015). If we enhance metallicity, we increase the strength of spectral lines, so that to the first order more lines get weakened in faculae and their contrast increases. Because the line density is higher in the UV, the increase in contrast is also greater there, as confirmed by Fig. 3b. In contrast, the spot contribution changes little (Fig. 3a). This can be understood by looking at the spectral profiles of the faculae and spot contributions to the brightness change. While the facular profile contains many spectral features brought about by the Fraunhofer lines, the spot profile is quite smooth. This indicates that the contrast due to Fraunhofer lines is predominant for the faculae component, while continuum plays a more important role for the spot component. This is supported by the temperature profile of sunspot umbrae and penumbra, which have similar (or flatter) gradients than the quiet Sun but a significantly lower effective temperature. Stellar photometric brightness variation measurements spanning a decade or more have predominantly been made in the Strömgren b and y filters. Thus the dependence of brightness change on metallicity in these filters, shown in Fig. 4, is of particular interest. The brightness change in these filters is also particularly sensitive to metallicity. This is partly because facular and sunspot variations nearly balance each other for solar metallicity, especially in Strömgren b. For $M/H = 0.2$, for example, the brightness change in the Strömgren filter b is increased by a factor of 10.6 relative to the Sun, whereas in the Strömgren filter y it is increased by a smaller but still sizeable factor of 1.86.

Interestingly, for metallicities smaller than in the Sun, the brightness change becomes negative in the Strömgren b filter, which indicates that for low metallicities the brightness changes over the activity cycle are spot-dominated rather than faculae-dominated. Both regimes have been observed in main-sequence stars (Radick et al. 1998; Lockwood et al. 2007; Montet et al. 2017), where magnetically less active and consequently older stars usually show a direct correlation between brightness and activity, i.e. they are faculae-dominated, while more active stars are spot-dominated. It was observationally established that the transition between these two regimes is approximately at a chromospheric activity of $\log R'_{\rm HK} \approx -4.7$, although the two regimes

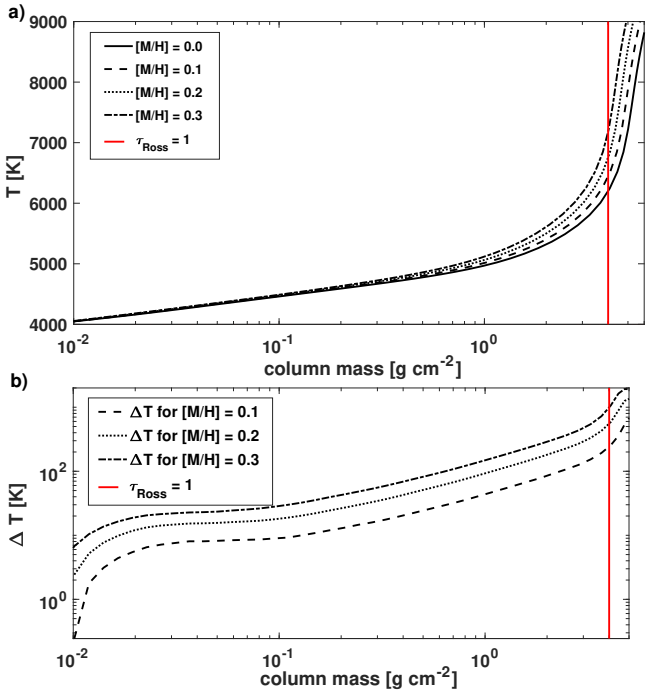

Fig. 5. Self-consistently calculated atmospheric models for different metallicities. All models are constructed for $T_{\rm eff}$ of the quiet sun model, which is $T_{\rm eff}$ = 5777 K. *Panel a*: temperature structure of quiet stellar region vs. column mass. *Panel b*: temperature change, ΔT, with respect to the solar metallicity value $M/H = 0.0$ with column mass. The red line indicates $\tau_{\rm Ross} = 1$ layer for the quiet Sun's ($M/H = 0.0$) atmosphere.

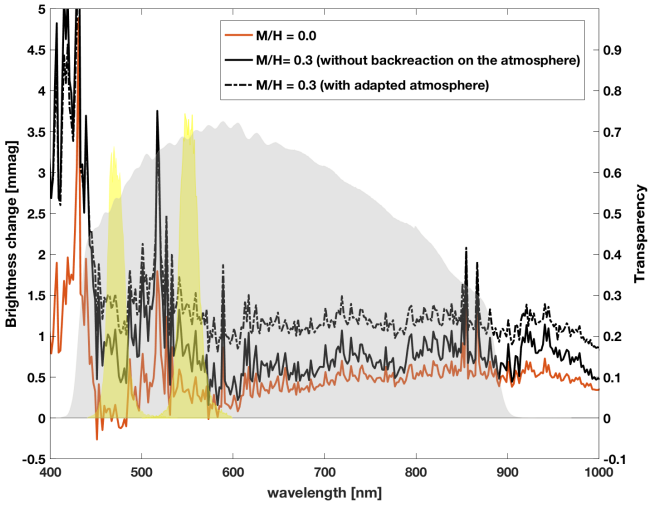

Fig. 6. Amplitude of solar cycle brightness change as defined in Fig. 2. Orange solid line: solar case ($M/H = 0.0$); black solid line: hypothetical Sun calculated with $M/H = 0.3$ using solar atmosphere models; black dotted line: same as before, but using atmospheric models consistently recalculated with $M/H = 0.3$, i.e. the back-reaction of the radiation field on the atmospheric structure, and continuum opacity change due to a different electron concentration are considered. The yellow and grey shaded areas are the same as in Fig. 2.

overlap (Montet et al. 2017). Our finding that a change in metallicity can lead to a change from faculae- to spot-dominated brightness variations for the same activity level is one possible explanation for this observation.

3.2. Adjusting atmospheric models to changed metallicity

While in Sect. 3.1 we focused on the effect of metallicity directly on the opacity of atomic and molecular lines, we did not take into account the change in the electron concentration that affects the H^- concentration and consequently the continuum opacities. Recalculating the overall electron concentration leads to a significant change in the radiation field and a shift in the continuum formation height, which results in a different effective temperature. In order to restore the initial effective temperature, we accounted for the changed radiation field by recalculating the atmospheric structure to be in radiative equilibrium. In this section the aim is to investigate all effects together, the Fraunhofer lines, recalculated electron concentrations, and the changed atmospheric structure for different metallicities in the range $-0.1 \leq M/H \leq 0.4$.

In order to quantify the full effect of metallicity on the brightness change of a star it is therefore necessary to recalculate models for the corresponding M/H value as described in Sect. 2.2. Models of the quiet stellar regions, umbra, and penumbra can be self-consistently calculated with ATLAS9 assuming radiative equilibrium and preserving their effective temperatures for a prescribed M/H value. In Fig. 5a the recalculated atmospheric structures for the quiet stellar regions are displayed for four different M/H values, whereas the resulting ΔT between a particular metallicity value and the solar case ($M/H = 0.0$) is shown in Fig. 5b. Focusing on the location of the Rosseland optical depth, $\tau_{\rm Ross} = 1$, in this plot shows that the greatest atmospheric changes of a few hundred K are at depths where the continuum is formed. This can be explained as follows. On the one hand, for increased metallicity spectral lines become stronger, the emerging radiation decreases, and so does $T_{\rm eff}$. To compensate for this decrease in emerging radiation, and to return to the initial $T_{\rm eff}$, in a self-consistent atmosphere the temperature of the continuum-forming layer has to be increased. The stronger continuum offsets the deeper spectral lines, so that $T_{\rm eff}$ remains unchanged. On the other hand, increased opacity due to higher metallicity leads to a slight shift in the $\tau_{\rm Ross} = 1$ on the column mass scale, so that the continuum is formed at somewhat higher layers compared to the solar case.

As the facular model is not in radiative equilibrium, it cannot be directly recalculated by the ATLAS9 code. Therefore, we assumed that a changed metallicity value has the same effect on the temperature structures of the faculae as on the quiet stellar regions, applying the ΔT shown in Fig. 5b to the solar facular model. In other words, we assumed that the change of the metallicity preserves the temperature contrast between the faculae and the quiet regions as a function of the column mass. We plan to test this assumption in future with a realistic 3D MHD calculation, which is, however, beyond the scope of the present paper. Taking all the combined effects into account has a large impact on stellar photometric brightness change, as shown by the difference between the solid black line and the dashed black line in Fig. 6. In this particular case, for a metallicity value of $M/H = 0.3$, the radiative flux difference between activity maximum and minimum in the Strömgren b and y filters is approximately 1.5 times greater when we consider recalculated and adjusted atmospheric models compared to the case considered in the previous Sect. 3.1.

Finally, the effect of metallicity on the brightness changes in the Strömgren b and y filters, and the *Kepler* pass-band is shown in Fig. 7. In this set of calculations the combined effect of lines, recalculated atmospheric model and changed electron concentration is captured. We note that the solar case is not the same

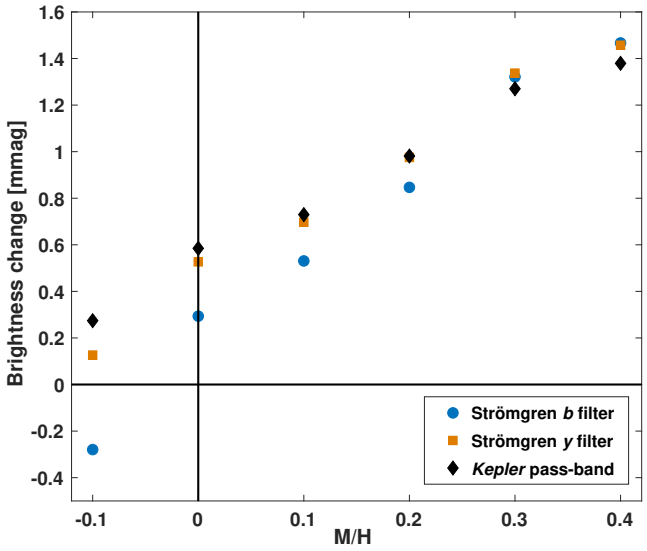

Fig. 7. Change in radiative flux integrated over Strömgren b and y filters and *Kepler* pass-band as a function of metallicity for cases with recalculated atmosphere models.

reference as in the previous section; Unruh et al. (1999) adjusted the temperature structure of the initial facular model for the solar case to match the observed emergent spectra without changing the electron concentration. Recalculating the electron concentration for the adjusted temperatures in the facular model leads to a greater brightness change and consequently a shifted reference point. The combined effect leads to an even stronger increase in brightness change with greater metallicity than was found in Sect. 3.1 for the isolated effect of metallicity on Fraunhofer lines. A transition to a spot-dominated regime is found for the Strömgren b filter close to $M/H = -0.1$, where a similar result was found in Sect. 3.1.

These findings support the hypothesis that the balance between radiation from dark and bright magnetic features that determines the brightness change on the magnetic activity cycle timescale is sensitive to stellar fundamental parameters. In particular, the solar metallicity value is close to a complete compensation regime, which is one possible explanation for the low brightness change of the Sun compared to other Sun-like stars of similar chromospheric activity (Lockwood et al. 2007, 2013). Previous analysis of the relationship between chromospheric activity measured in $\log R'_{\rm HK}$ and photometric variations in Strömgren $(b + y)/2$ for Sun-like stars revealed a power-law relation (Lockwood et al. 1992, 2007). The Sun, however, was found to be located significantly below the established power-law relation (Lockwood et al. 2007; Shapiro et al. 2014; Radick et al. 2018). According to our calculations a hypothetical Sun with a metallicity of $M/H = 0.4$ would have photometric variations for $(b+y)/2$ of log rms $= 0.52 \times 10^{-3}$, and thus would lie close to the power-law relation found by (Lockwood et al. 2007, their Fig. 7).

3.3. Inclination effects

The Sun is always observed from a close to an equator-on vantage point. This is different for other stars, which are observed at random inclination angles, defined as the angle between the observer's viewing direction and the rotational axis of the star. We define the inclination angle such that a pole-on view corresponds to 0° and an equator-on view to 90°. Several investigations have studied the effect of inclination on the solar brightness variation on the magnetic activity cycle timescale (e.g. Schatten 1993; Knaack et al. 2001; Shapiro et al. 2014). All previous studies found that an inclined Sun would show a greater brightness variation, although they differed in the magnitude of the effect of inclination. However, prior studies considered only the solar case, and did not consider other stellar fundamental parameters. Here we investigate the effect of the inclination for stars with different metallicities; our focus is on the brightness change in the Strömgren b and *Kepler* filters. Using the calculated spectra for different metallicities with the recalculated model (see Sect. 3.2), the brightness changes were obtained for different view angles.

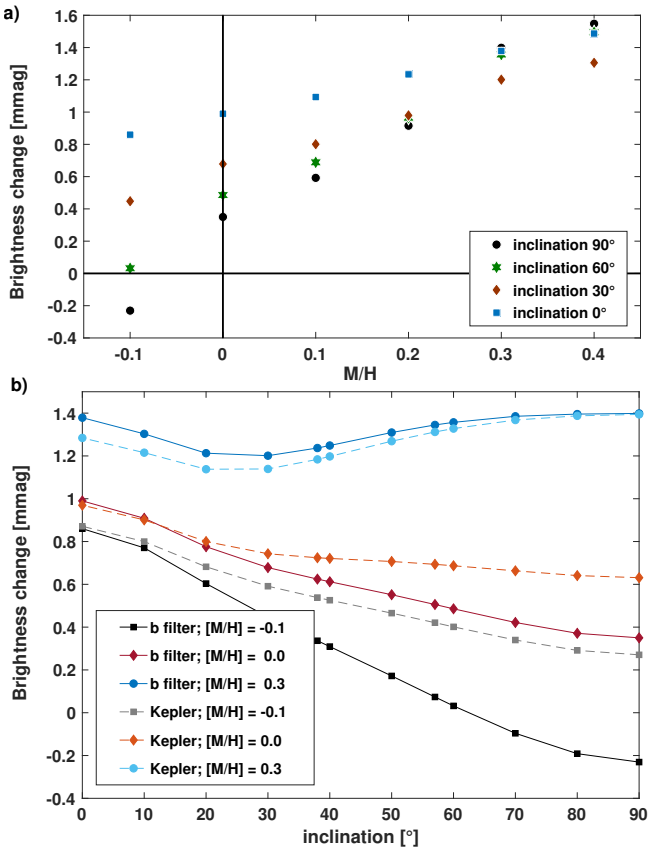

Fig. 8. Brightness change in the Strömgren b and *Kepler* filters for different inclination angles (90° corresponds to an equator-on view) and different metallicity values. *Panel a*: brightness change vs. metallicity for four different inclination angles. *Panel b*: brightness change vs. inclination angle for three different metallicities and two different filters (Strömgren b and *Kepler*).

Figure 8a shows the brightness change with the metallicity for four inclination angles $\alpha = [0°, 30°, 60°, 90°]$. It is evident that for metallicity values between $M/H = -0.1$ and $M/H = 0.2$ the brightness change increases with decreasing inclination. With increasing M/H values the effect of inclination diminishes. The dependence on the inclination is more complex for metallicities greater than $M/H = 0.2$. We note that our result for different inclinations of the solar case is in agreement with previous investigations (Radick et al. 1998; Knaack et al. 2001; Shapiro et al. 2014). Therefore, we conclude that the brightness change in stars with different fundamental parameters can show different dependences on inclination. This is illustrated in Fig. 8b, where the brightness change with inclination is shown for three metallicity values. For $M/H = 0.3$, starting from the equator-on view, the

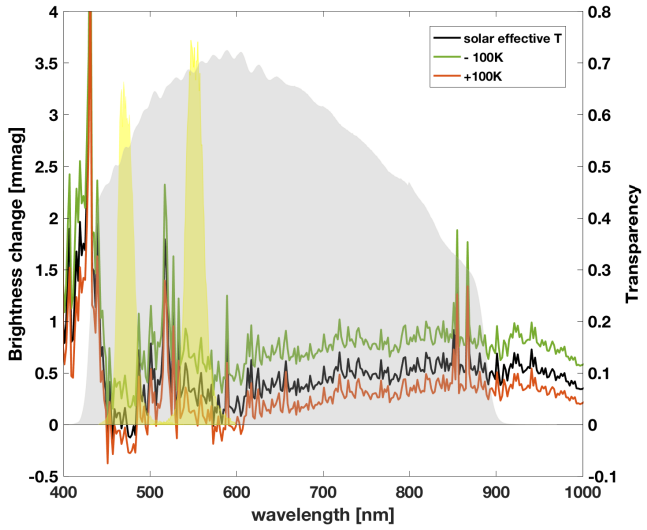

Fig. 9. Amplitude of solar cycle brightness change as defined in Fig. 2. Black line: solar case with solar effective temperatures for all features; green line: hypothetical Sun, but with $T_{\rm eff}$ reduced by 100 K for all components; orange line: same as before, but with $T_{\rm eff}$ increased by 100 K for all components.

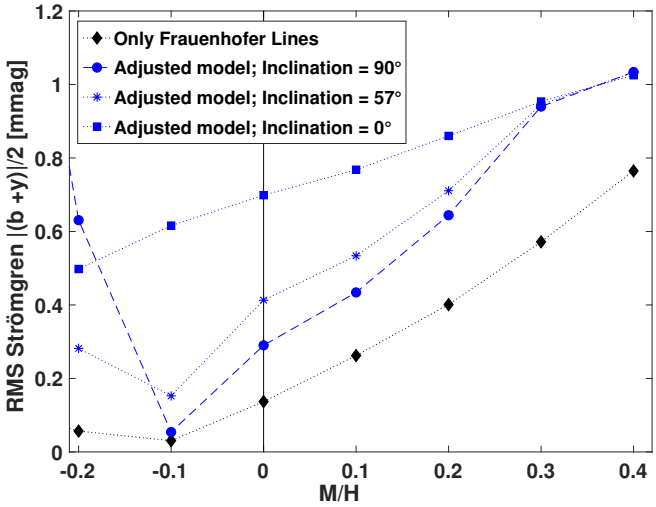

Fig. 10. Estimated rms of the radiative flux change in the Strömgren $(b+y)/2$ filters for four different cases vs. metallicity. Black: only the effect of the Fraunhofer line on the opacity is considered; blue: recalculated atmosphere models are used.

brightness change in the Strömgren b filter (Fig. 8b) decreases first with decreasing inclination angle. Then, at lower inclination angles the brightness change increases again towards a pole-on view. This is explained in more detail in Appendix A, where we discuss the CLVs of faculae.

3.4. Effective temperature

So far we have only studied the effect of metallicity. Another important fundamental stellar parameter that likely affects stellar brightness change is the effective temperature. To understand the role of the effective temperature, the brightness change was calculated for effective stellar temperatures of 100 K below and 100 K above the solar value. Such small deviations from the solar value are of special interest as the measurement accuracy of this parameter is approximately 100 K (Pinsonneault et al. 2012).

The atmospheric models for different effective temperatures were recalculated following the same procedure as described in Sect. 2.2. Subsequently, the brightness change was calculated with SATIRE. Figure 9 shows the total brightness change for the three considered $T_{\rm eff}$ values. Already a 100 K decrease in $T_{\rm eff}$ causes the brightness change to increase remarkably, while a similar increase in $T_{\rm eff}$ lowers the brightness change and leads to a spot-dominated cycle in the Strömgren b filter (for solar M/H). Such a sensitive response to a slight change in the effective temperature emphasises the special combination of stellar parameters of our Sun.

3.5. Towards observational quantities

Having investigated the effect of metallicity on the spectral brightness change, together with the effect of the inclination, we now link our comprehensive theoretical results to observed stellar photometric brightness changes. Observed stellar photometric brightness variations are usually analysed in the Strömgren b and y filters separately or as one averaged quantity over Strömgren $(b+y)/2$ (Lockwood et al. 2007, 2013; Radick et al. 2018). Furthermore, observational studies also quantify the brightness change as the root mean square (rms) variation of the annual mean magnitudes that are obtained from long-term observations. However, for our model we considered the brightness difference between the magnetic cycle maximum and minimum of only one cycle, which means that a one-to-one comparison cannot be made in a straightforward manner.

We approximated the rms variation for Strömgren $(b+y)/2$ by using the relation rms $= A/\sqrt{2}$, where A is the amplitude of a sine function. Figure 10 shows the rms variations obtained in this way versus metallicity. We note that the absolute value of the brightness change was considered, i.e. the phase at which maximum brightness is reached was neglected. Overall, Fig. 10 shows that photometric brightness variation for Strömgren $(b+y)/2$ is close to a local minimum for solar metallicity and inclination. The same holds for solar metallicity and inclination angles up to roughly 60°, and for the brightness change in the Strömgren b filter (see Figs. 4, 7, and 8). The smallest rms variations among the computed cases is found for metallicity $M/H = -0.1$. Combining this with the results of the effective temperature study reveals that the photometric brightness variations in the Strömgren b, and Strömgren $(b+y)/2$ filter for the solar case is close to a local minimum for the parameter space of the metallicity and effective temperature.

4. Conclusions

Physics-based models are of importance for a comprehensive understanding of long-term stellar and solar brightness variations, but to date have rarely been applied to stars other than the Sun. Of special interest is the long-standing puzzle that solar brightness variability on the timescale of the 11 year activity cycle appears anomalously low in comparison to variability of Sun-like stars with a near-solar level of magnetic activity. Such models are also of importance for the detection of extra solar planets (see e.g. Borgniet et al. 2015). Thus, there has been a drive towards understanding the solar–stellar connection, especially after the launch of the Corot (Bordé et al. 2003; Baglin et al. 2006) and *Kepler* (Borucki et al. 2010) space missions that provide broadband stellar photometry of unprecedented precision. In addition, detailed models of stellar

variability are of interest for the upcoming TESS (Ricker et al. 2015; Lund et al. 2017) and PLATO (Catala 2009; Rauer et al. 2016) missions.

In this study we extended the well-established solar variability model (SATIRE) to stars with different fundamental parameters. For this we kept the distribution of magnetic features fixed, but we calculated the emergent intensities for different values of metallicity and effective temperatures. In a first step, we demonstrated that changing metallicity affects the Fraunhofer lines in quiet stellar regions in a different way than in faculae. In particular, we find that higher metallicity values result in a significant increase in contrasts of faculae, i.e. bright magnetic features. The enhanced contrasts lead to a greater amplitude in the photometric brightness change over a magnetic activity cycle. While isolating the effect of Fraunhofer lines on the brightness change confirmed their important contribution, which was first established for the solar case (Shapiro et al. 2015), it is crucial to account for the back-reaction of the changed radiation field on the atmospheric structure. In a self-consistent approach, the brightness change is affected by metallicity such that even small changes in metallicity values have a significant impact on stellar brightness change for pass-bands used in space- and ground-based stellar observations. Furthermore, examining the brightness changes for a hypothetical Sun with slightly changed effective temperature in both directions reveals an increase in brightness change for the Strömgren *b* filter.

All in all, we conclude that the combination of the solar fundamental parameters corresponds to a local minimum in the brightness change in the Strömgren filters on the solar cycle timescale. This finding thus explains the anomalously low solar brightness change by the incidental combination of fundamental solar parameters (Shapiro et al. 2016). This is a plausible explanation for low solar brightness change. In addition, a possible observational bias hinders the identification of stars with low brightness change, and thus potential solar twins.

We also find that the inclination does not have a strong impact on the brightness change for stars with metallicities somewhat higher than solar. Due to the dependence of CLVs on metallicity, a star with double the metallicity of the Sun would show almost no difference in the brightness changes when it is observed equator-on or pole-on. In contrast, inclination angles play an important role for stars with low metallicity (approximately $M/H = 0.2$ or lower). For stars with lower metallicity than in the Sun, different inclination angles can even lead to a transition from faculae-dominated to spot-dominated brightness changes. While this result confirms previous investigations on the importance of the inclination for solar metallicity, it additionally reveals that the inclination effect becomes weaker for stars with higher metallicities.

In the future, our theoretical findings will be tested against observational data. Recently, sufficient observational data were obtained for one Sun-like star to perform an extensive analysis. The star HD 173701, whose metallicity is twice as high as the solar value, shows higher chromospheric variation, but an even higher photometric brightness variation. Both effects can be explained by the difference in the metallicity (Karoff et al. 2018). Another curious case is the Sun-like star HD 143761, which has a near-solar effective temperature but whose metallicity is half of the solar value (von Braun et al. 2014). This star shows a photometric variability that is spot-dominated, despite being less active than the Sun (Radick et al. 2018). Such a rule-breaking behaviour can be explained by a lower facular contrast due to its low metallicity, which is in line with our results. We note, however, that this example should be treated with caution since observational data with two different instruments detected a change from correlated to anticorrelated behaviour (Radick et al. 2018). Unfortunately, for more detailed comparisons we lack a complete set of measurements to determine accurate fundamental parameters of many of the observed main-sequence stars with observed brightness variations on activity cycle timescales. Therefore, an effort is currently underway to obtain a more complete set of observations, including accurate measurements of stellar fundamental parameters and long-term variability for an extended number of *Kepler* stars (Petigura et al. 2017; Kong et al., in prep.) for comparison between modelling and measurements.

We conclude that the complex interaction between radiation and matter is crucial in order to obtain correct brightness variation calculations. However, since the model adjustment uses simplified assumptions and cannot account for 3D effects, 3D MHD calculations are needed for a more realistic approach. These simulations can provide a more realistic modelling for their brightness changes using a 1.5D approach (Norris et al. 2017). Unfortunately, current 3D MHD calculations are only available for different effective temperatures on a coarse grid (Beeck et al. 2015). Consequently, we aim to obtain 3D MHD simulations on a finer effective temperature grid together with different metallicity cases and to compute the entire spectrum in order to study the dependence of stellar brightness changes on the fundamental stellar parameters.

Acknowledgements. We thank Jeff Hall for encouraging and useful discussions. This work has received funding from the European Research Council (ERC) under the European Union's Horizon 2020 research and innovation programme (grant agreement No. 715947). This work has been partially supported by the BK21 plus programme through the National Research Foundation (NRF) funded by the Ministry of Education of Korea. WS acknowledges travelling support by the grant 200020-169647 of the Swiss National Science Foundation.

References

Anders, E., & Grevesse, N. 1989, Geochim. Cosmochim. Acta, 53, 197
Anderson, R. I., Reiners, A., & Solanki, S. K. 2010, A&A, 522, A81
Baglin, A., Auvergne, M., & Boisnard, L. 2006, in 36th COSPAR Scientific Assembly, COSPAR Meeting, 36
Baliunas, S. L., Donahue, R. A., Soon, W. H., et al. 1995, ApJ, 438, 269
Beeck, B., Schüssler, M., Cameron, R. H., & Reiners, A. 2015, A&A, 581, A42
Böhm-Vitense, E. 1958, Z. Astroph., 46, 108
Bordé, P., Rouan, D., & Léger, A. 2003, A&A, 405, 1137
Borgniet, S., Meunier, N., & Lagrange, A.-M. 2015, A&A, 581, A133
Borucki, W. J., Koch, D., Basri, G., et al. 2010, Science, 327, 977
Castelli, F. 2005, Mem. Soc. Astron. It. Suppl., 8, 34
Castelli, F., & Kurucz, R. L. 1994, A&A, 281, 817
Catala, C. 2009, Exp. Astron., 23, 329
Ermolli, I., Matthes, K., Dudok de Wit, T., et al. 2013, Atm. Chem. Phys., 13, 3945
Fligge, M., Solanki, S. K., & Unruh, Y. C. 2000, A&A, 353, 380
Fontenla, J. M., Avrett, E. H., & Loeser, R. 1993, ApJ, 406, 319
Fontenla, J. M., Avrett, E., Thuillier, G., & Harder, J. 2006, ApJ, 639, 441
Hall, J. C., Henry, G. W., Lockwood, G. W., Skiff, B. A., & Saar, S. H. 2009, AJ, 138, 312
Judge, P. G., Lockwood, G. W., Radick, R. R., et al. 2012, A&A, 544, A88
Karoff, C., Metcalfe, T. S., Santos, Ângela R. G., et al. 2018, ApJ, 852, 46
Knaack, R., Fligge, M., Solanki, S. K., & Unruh, Y. C. 2001, A&A, 376, 1080
Krivova, N. A., Solanki, S. K., Fligge, M., & Unruh, Y. C. 2003, A&A, 399, L1
Kurucz, R. L. 1992, Rev. Mex. Astron. Astrofis., 23, 45
Lanza, A. F., Pagano, I., Leto, G., et al. 2009, A&A, 493, 193
Lean, J., Skumanich, A., & White, O. 1992, Geophys. Res. Lett., 19, 1591
Lemaire, P., Gouttebroze, P., Vial, J. C., & Artzner, G. E. 1981, A&A, 103, 160
Lockwood, G. W., Henry, G. W., Hall, J. C., & Radick, R. R. 2013, in New Quests in Stellar Astrophysics III: A Panchromatic View of Solar-Like Stars, With and Without Planets, eds. M. Chavez, E. Bertone, O. Vega, & V. De la Luz, ASP Conf. Ser., 472, 203
Lockwood, G. W., Skiff, B. A., Baliunas, S. L., & Radick, R. R. 1992, Nature, 360, 653

Lockwood, G. W., Skiff, B. A., Henry, G. W., et al. 2007, ApJS, 171, 260
Lund, M. N., Handberg, R., Kjeldsen, H., Chaplin, W. J., & Christensen-Dalsgaard, J. 2017, Eur. Phys. J. Web Conf., 160, 01005
Mitchell, Jr., W. E., & Livingston, W. C. 1991, ApJ, 372, 336
Montet, B. T., Tovar, G., & Foreman-Mackey, D. 2017, ApJ, 851, 116
Norris, C. M., Beeck, B., Unruh, Y. C., et al. 2017, A&A, 605, A45
Petigura, E. A., Howard, A. W., Marcy, G. W., et al. 2017, ApJ, 154, 107
Pinsonneault, M. H., An, D., Molenda-Żakowicz, J., et al. 2012, ApJS, 199, 30
Radick, R. R., Lockwood, G. W., Skiff, B. A., & Baliunas, S. L. 1998, ApJS, 118, 239
Radick, R. R., Lockwood, G. W., Henry, G. W., Hall, J. C., & Pevtsov, A. A. 2018, ApJ, 855, 75
Rauer, H., Aerts, C., Cabrera, J., & PLATO Team 2016, Astron. Nachr., 337, 961
Ricker, G. R., Winn, J. N., Vanderspek, R., et al. 2015, Instrum. Syst., 1, 014003
Schatten, K. H. 1993, J. Geophys. Res., 98, 18
Shapiro, A. I., Schmutz, W., Rozanov, E., et al. 2011, A&A, 529, A67
Shapiro, A. I., Solanki, S. K., Krivova, N. A., et al. 2014, A&A, 569, A38
Shapiro, A. I., Solanki, S. K., Krivova, N. A., Tagirov, R. V., & Schmutz, W. K. 2015, A&A, 581, A116
Shapiro, A. I., Solanki, S. K., Krivova, N. A., Yeo, K. L., & Schmutz, W. K. 2016, A&A, 589, A46
Solanki, S. K. 1993, Space Sci. Rev., 63, 1
Solanki, S. K., Inhester, B., & Schüssler, M. 2006, Rep. Prog. Phys., 69, 563
Solanki, S. K., Krivova, N. A., & Haigh, J. D. 2013, ARA&A, 51, 311
Steiner, O. 2005, A&A, 430, 691
Unruh, Y. C., Solanki, S. K., & Fligge, M. 1999, A&A, 345, 635
Unruh, Y., Solanki, S., & Fligge, M. 2000, Space Sci. Rev., 94, 145
Vernazza, J. E., Avrett, E. H., & Loeser, R. 1981, ApJS, 45, 635
Vieira, L. E. A., Norton, A., Dudok de Wit, T., et al. 2012, Res. Lett., 39, L16104
von Braun, K., Boyajian, T. S., van Belle, G. T., et al. 2014, MNRAS, 438, 2413
Wilson, O. C. 1978, ApJ, 226, 379
Yeo, K. L., Solanki, S. K., & Krivova, N. A. 2013, A&A, 550, A95
Yeo, K. L., Solanki, S. K., & Norris, C. M. et al. 2017, Phys. Rev. Lett., 119, 091102

Appendix A: Dependence of brightness change on inclination and CLV

To understand why the dependence of brightness change on the inclination itself depends on metallicity, we investigate the CLV of facular contrast. Figure A.1 shows the CLV of the facular contrast in the Strömgren b filter and the *Kepler* pass-band for the solar case, and the case with $M/H = 0.3$. These two cases represent the two different types of behaviour discussed in Sect. 3.3. The facular contrast is multiplied by the corresponding μ to account for the foreshortening effect. For the solar case, the facular contrast increases from the disc centre outwards. Since this increase continues almost to the edge of the disc, a relocation of the faclulae towards the centre will result in only a slight decrease in the contrast with inclination. Thus, the effect of the brightness change is weak (see Fig. A.2a).

For greater metallicity, the facular contrast in the middle of the disc is almost constant, while a steep drop starts at $r/R \approx 0.7$. The difference between the facular contrast around the disc centre and the limb is significantly greater than for the solar case. Therefore, two contributions compete in the brightness change when the star with higher metallicity is inclined towards the pole-on view. With inclination some of the faculae are seen closer to the disc centre where the facular contrast does not change, others are shifted to the limb where the facular contrast drops significantly. Therefore, the facular brightness change decreases greatly with inclination for a metallicity value of 0.3 (see Fig. A.2b).

To explain the different behaviour with inclination for metallicity values in the range $-0.1 < M/H \leq 0.2$ and metallicity values greater than 0.2, we plot the facular and spot brightness changes with different inclinations for the solar value ($M/H = 0.0$) and the metallicity value $M/H = 0.3$ in Fig. A.2. For the solar case, the facular brightness change decreases somewhat with inclination, at the same time spot brightness change decreases by a much larger amount, so that total brightness change goes up. For the $M/H = 0.3$ the brightness change due to spots drops with inclination by a similar amount to that for $M/H = 0$, but at the same time facular brightness change drops by a similar amount, or even slightly more, so that the balance between faculae and spots remains either the same or is only slightly shifted towards the spot contribution. Consequently, the total brightness change either remains the same or decreases.

While the total surface area covered by magnetic features remains constant when the star is inclined, due to the equatorial symmetry of the distributions, the location of magnetic features on the disc changes. Thus, the contrasts of the faculae and spots are modified. Consequently, the total brightness change is altered due to a changed balance of facular and spot contributions. For the solar metallicity value the faculae contribution decreases slightly with decreasing inclination, i.e. towards a pole-on view, but at the same time the negative contribution of the spots increases significantly. This leads to an increase in the total brightness change. We find the opposite behaviour for metallicity values greater than $M/H = 0.2$. For these cases the facular contrast decreases significantly with inclination, while the spot contrast behaves almost as for the solar metallicity value. This results in a decrease in the overall brightness change with inclination.

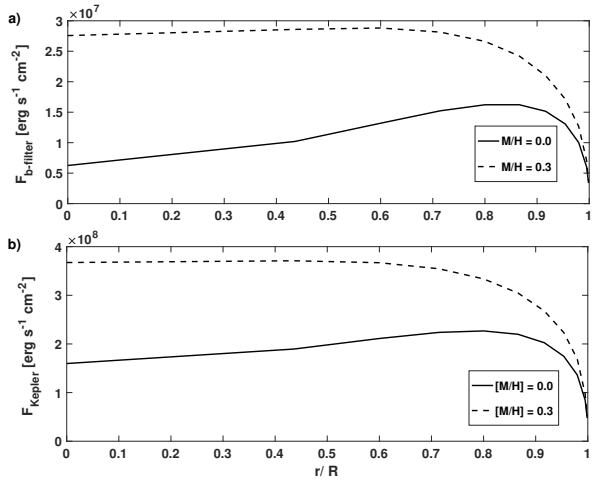

Fig. A.1. Centre-to-limb variation of facular flux difference. Here r/R is the normalised radial distance from the centre of the stellar disc. Two flux differences for metallicities are shown: the solar value $M/H = 0.0$ and $M/H = 0.3$: *panel a*: flux differences in the Strömgren b filter and *panel b*: in the *Kepler* pass-band.

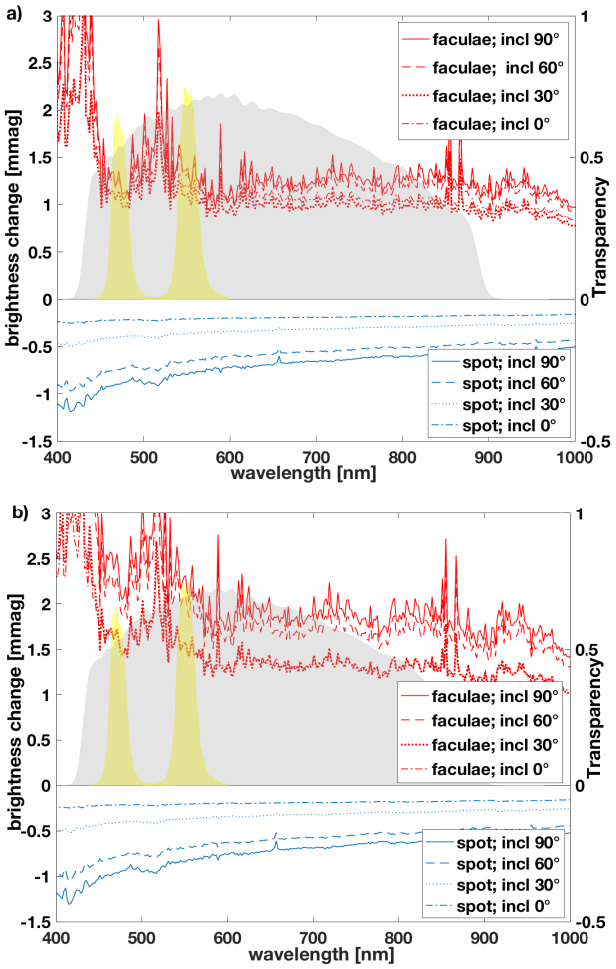

Fig. A.2. Brightness change for different components at different inclination angles for two metallicity values M/H: *panel a*: for the solar case $M/H = 0.0$ the facular (red) and spot (blue) contributions for different inclinations; *panel b*: for $M/H = 0.3$ the facular (red) and spot (blue) contributions for different inclinations.